Passive Cooling Method Analysis & Optimization of PV Solar Panel Heat Sink

Manish Singh[1], Kamlesh Kumar Ratre[2]

[1]M. Tech Scholar, Department of Mechanical Engineering, VEC Ambikapur, C.G., India
[2]Assistant Professor, Department of Mechanical Engineering, VEC Ambikapur, C.G. India

Abstract

The development of solar photovoltaic (PV) systems in arid climates is hindered primarily by high temperatures, which adversely affect system performance and lifespan. This manuscript presents a comprehensive approach to address this challenge by developing an analytical model for predicting the temperature of PV panels under a passive cooling system specifically designed for arid environments. The analytical model takes into account the crucial relationship between solar panel temperature and its conversion efficiency. By applying Kirchhoff's and Ohm's laws for a complex circuit, the model accurately calculates the heat flux within the solar panel system, allowing for the determination of temperatures for each layer in the system.

The study deduces closed-form analytical expressions that describe the temperature, output power, and conversion efficiency of the solar panel as functions of various factors, including solar irradiance, ambient temperature, emissivity, wind velocity, tilt angle, and dimensions of fins. These expressions provide valuable insights into the thermal behaviour of the system and enable the evaluation of its performance under different environmental conditions.

Keywords: PV solar panels, Thermal management systems, Thermal performance, Cooling efficiency, Temperature, Energy conversion efficiency, Passive cooling, Active cooling, Forced convection, Liquid cooling.

1. Introduction

The increasing demand for renewable energy sources has resulted in a significant rise in the use of photovoltaic (PV) solar panels. However, the efficiency of solar panels is highly affected by temperature, leading to a decrease in their overall output. Therefore, proper cooling mechanisms are crucial for maintaining the efficiency of solar panels. One effective method is using heat sinks.

One common cooling method is the use of a heat sink, which is a component designed to dissipate heat by transferring it to a surrounding medium, such as air or water. The effectiveness of a heat sink is determined by various factors, including the material properties, design, and operating conditions. PV panels convert sunlight into electrical energy, providing an environmentally friendly alternative to traditional energy sources. However, the performance and lifespan of PV systems are significantly affected by the operating temperature, particularly in arid climates.

High temperatures pose a primary challenge to the development and efficient operation of PV systems in arid regions. As the temperature rises, the performance of PV panels diminishes, leading to reduced power output and a shortened lifespan. It becomes crucial to develop effective cooling strategies to

mitigate the adverse effects of high temperatures and maintain the operating temperature within an acceptable range.

The goal of this thesis is to address the challenge of high temperature in solar PV systems by developing an analytical model to predict the temperature of PV panels under a passive cooling system in an arid environment. By accurately estimating the temperature of the panels, it becomes possible to assess their efficiency and power output, as well as evaluate the impact of various environmental factors and design parameters. The proposed analytical model builds upon fundamental principles such as Kirchhoff's and Ohm's laws for a complex circuit to calculate the heat flux within the PV panel system. By considering the link between solar panel temperature and conversion efficiency, the model provides closed-form analytical expressions for temperature, output power, and conversion efficiency as functions of solar irradiance, ambient temperature, emissivity, wind velocity, tilt angle, and dimensions of fins.
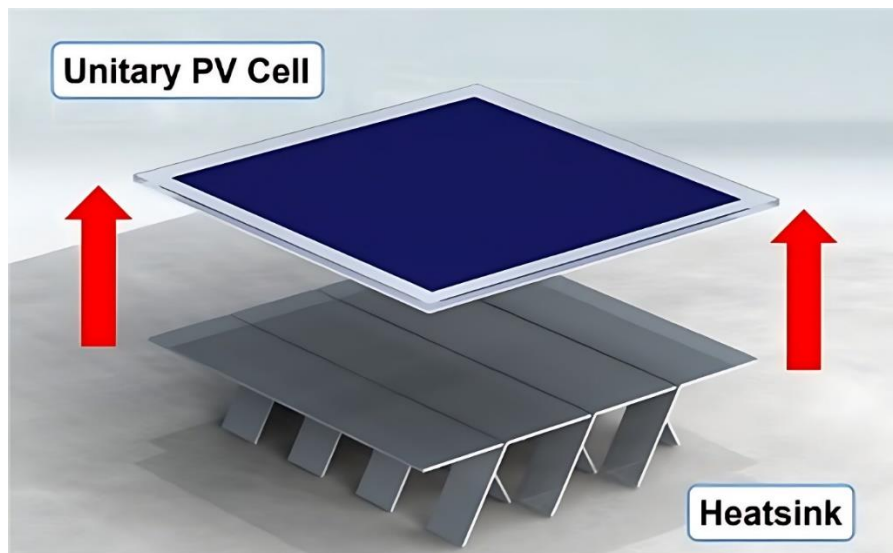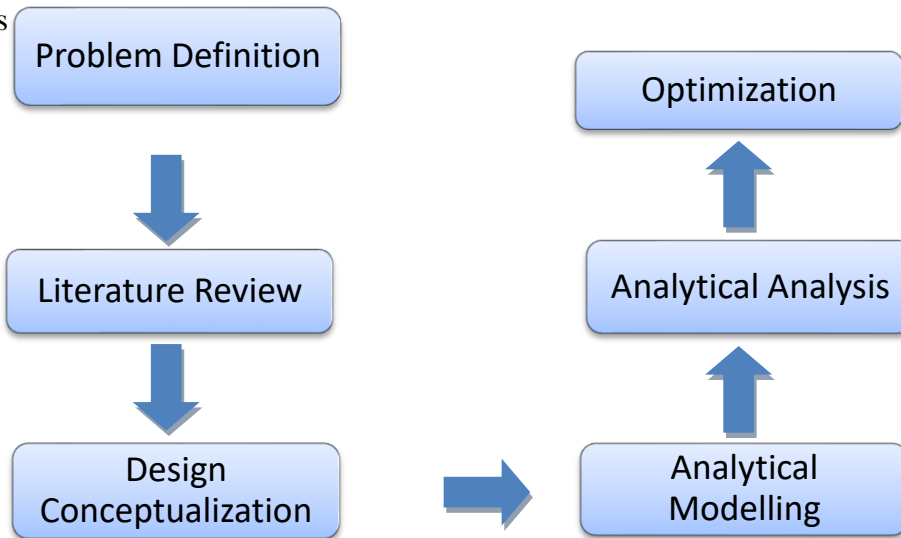

Figure 1: Solar Panel With Heat Sink

To validate the accuracy and effectiveness of the developed model, a comparison is made with existing results from the literature. Furthermore, the thesis also investigates the required length of fins for ensuring the safe thermal operation of solar panels in harsh desert environments.

By providing a comprehensive understanding of the operating temperature and efficiency of PV panels in arid climates, this thesis contributes to the development of sustainable and efficient solar PV systems. The insights gained from the analytical model can inform the design and optimization of cooling strategies, thereby enhancing the performance and longevity of PV systems operating in challenging desert environments.

2. Methodology

The methodology for designing and optimizing a composite material heat sink for solar panel cooling typically involves

```
Problem Definition
        ↓
Literature Review
        ↓
Design Conceptualization  →  Analytical Modelling  ↑  Analytical Analysis  ↑  Optimization
```

2.1 Heat sink design and optimization techniques

Heat sink design and optimization techniques play a crucial role in ensuring efficient cooling of solar panels. Some commonly used techniques include:

a) **Fin Design:**

This involves adding fins to the heat sink to increase the surface area and enhance heat dissipation. A fin design is a common technique used in heat sink design to increase the surface area and enhance heat transfer. Fins are thin projections or extensions from the main body of the heat sink, which can be attached to the base or to the heat pipes. The aim of using fins is to increase the heat transfer coefficient, thereby improving the overall performance of the heat sink.

There are different types of fin designs, such as straight fins, pin fins, helical fins, tapered fins, and wavy fins. Straight fins are the simplest type and are commonly used in heat sinks. Pin fins are smaller and are used in compact heat sinks. Helical fins have a twisted shape and are useful for applications where airflow is limited. Tapered fins are wider at the base and thinner at the tip, which improves heat transfer. Wavy fins have a sinusoidal shape and are useful for low airflow conditions.

The design of the fin geometry depends on various factors such as the heat sink material, the cooling medium, the operating conditions, and the performance requirements. The optimization of the fin design involves determining the optimal size, shape, and spacing of the fins to maximize the heat transfer coefficient and minimize the pressure drop.

Numerical simulations using computational fluid dynamics (CFD) software can be used to predict the performance of different fin designs and optimize the fin geometry. The use of CFD analysis allows for the exploration of a wide range of design options and reduces the need for costly and time-consuming experimental testing.

The use of a well-designed fin configuration can significantly improve the heat transfer performance of a heat sink, resulting in better cooling of the solar panel and improved energy conversion efficiency.

b) **Material Selection:**

The choice of material used in the heat sink affects its thermal conductivity, weight, and cost. Carbon fiber and aluminum-based composites are popular materials for heat sink design due to their high thermal conductivity and low weight.

c) **Computational Fluid Dynamics (CFD) Simulation:**

CFD simulations can be used to predict the temperature distribution within the solar panel and heat sink system, and optimize the design for improved cooling performance.

d) **Optimization Algorithms:**

Various optimization algorithms can be used to find the optimal design parameters for the heat sink, such as fin geometry, material thickness, and fluid flow rate.

e) **Heat Pipe Technology:**

Heat pipes can be used in conjunction with heat sinks to improve the efficiency of the cooling system by transferring heat from the solar panel to the heat sink more effectively.

f) **Additive Manufacturing:**

Additive manufacturing techniques such as 3D printing can be used to create complex geometries and improve the performance of the heat sink.

A combination of these techniques can be used to design and optimize a composite material heat sink for efficient cooling of solar panels.

3. Problem Geometry and Description

The PV-HS (PV panel with heat sink cooling) system comprises multiple layers and different materials, each with unique thermal properties and thicknesses. The front and back surfaces of the system are directly exposed to the surrounding environment. Figure 1 illustrates the configuration of the considered system, and Table 1 provides information about the properties of the various layers of the PV panel.

To develop an innovative analytical model for predicting the temperature of the solar panel, the following assumptions were made:

1. Uniform Solar Irradiance: The solar irradiance is assumed to be the same for all cells in the PV panel. This implies clear skies without clouds or dust on the front surface of the panel.

2. Steady-State Heat Flow: The time response of the system is considered to be short, allowing for the assumption of steady-state heat flow. This assumes that the temperature distribution within the system remains constant over time.

3. Adiabatic Side Walls: The side walls of the PV-HS system are assumed to be adiabatic, meaning no heat transfer occurs through them. This simplifies the analysis by focusing on the front and back surfaces of the system.

4. One-Dimensional Flow: The thickness of the system is significantly smaller compared to its length and width. Consequently, the heat flow is assumed to be one-dimensional, simplifying the analysis to a single direction.
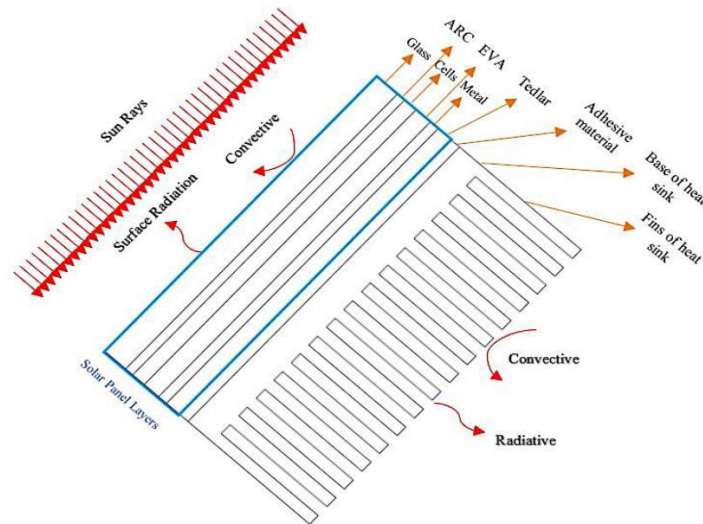
Figure 2: Layout of the photovoltaic (PV) panel with the considered cooling system

By making these assumptions, the analytical model aims to provide a comprehensive understanding of the temperature distribution within the PV panel and its interaction with the heat sink. This model facilitates the prediction of the operating temperature and helps evaluate the effectiveness of the cooling system in maintaining the desired temperature range.

Table 1: Properties of the layers of the PV panel

Layer	Thickness (mm)	Thermal Conductivity (W/m K)
Glass	3	1.8
ARC	0.0001	32
PV cells	0.225	148
EVA	0.5	0.35
Rear contact	0.01	237
Tedlar	0.01	0.2
Adhesive material	0.1	1.5
Heat sink	0.5	205

4. Mathematical Formulation and Analytical Solution

When sunlight reaches the front surface of the solar panel, a fraction is reflected, while the majority passes through to the solar cell layer. In this layer, some of the light energy is converted into electrical energy, while the remainder is converted to heat. The heat generated is dissipated to the environment through both the front and back sides of the panel.

By employing Ohm's and Kirchhoff's laws as an analogy, the total heat flow of the solar panel can be expressed as the sum of the heat flows from the front side (Q1) and the back side (Q2), as depicted in Figure 3. The equation for the total heat flow is as follows:

$$Q_t = Q_1 + Q_2 = I \times A \times (1 - \eta) \times \alpha_{abs} \times \tau_{tran} \qquad \text{......Equation 1}$$

Here,

I = represents the incident light intensity,

A is the solar panel area,

η is the panel efficiency,

α_{abs} is the absorptivity of the solar cell, and

τ_{tran} is the transmissivity of the glass cover.

The solar cell efficiency decreases linearly with the operating temperature, and this decrement rate depends on the PV material used. Existing literature presents various correlations expressing cell efficiency as a function of the efficiency at the lab reference temperature, material properties, and operating temperature. One such correlation, proposed by Evans and Florschuetz (1977), is given by:

$$\eta = \eta T,_{ref} \left[1 - \beta_{ref} \left(T_{ref} - T_{solar} \right) \right] \qquad \ldots\ldots\text{Equation 2}$$

In this equation,

$\eta T,_{ref}$ = represents the efficiency at standard test conditions (STC),

β_{ref} = is the temperature coefficient at STC, and

T_{ref} = is the reference test temperature.

To estimate the temperature of the solar panel (T_{solar}), two approaches can be used: one based on the heat flow from the front side and the other based on the heat flow from the back side. The equations for these approaches are:

$$T_{solar} = Q_1 \times \Sigma R_{th(f)} + T_{amb} \qquad \ldots\ldots\text{Equation 3}$$
$$T_{solar} = Q_2 \times \Sigma R_{th(b)} + T_{amb} \qquad \ldots\ldots\text{Equation 4}$$

Here,

$\Sigma R_{th(f)}$ = represents the total thermal resistance at the front side,

$\Sigma R_{th(b)}$ = is the total thermal resistance at the back side, and

T_{amb} = is the ambient temperature.

By substituting Equation (3) into Equation (4), we obtain the following expression:

$$Q_2 \times \Sigma R_{th(b)} = Q_1 \times \Sigma R_{th(f)} \qquad \ldots\ldots\text{Equation 5}$$

Using Equation (1) and substituting in Equation (5)

$$Q_1 = \frac{\Sigma R_{th(b)}}{\Sigma R_{th(f)}} Q_t - \frac{\Sigma R_{th(b)}}{\Sigma R_{th(f)}} Q_1 \qquad \ldots\ldots\text{Equation 6}$$

The expression of the heat flow of the front side as a function of the total heat is:

$$Q_1 = \left\{ \frac{\Sigma R_{th(b)}}{\Sigma R_{th(f)} + \Sigma R_{th(b)}} \right\} Q_t \qquad \ldots\ldots\text{Equation 7}$$

Using Equations (1), (2), and (7), and substituting into Equation (3) we can express the solar panel temperature as:

$$T_{solar} = \frac{\phi \times \left(1 - \eta T,_{ref}\left[1 - \beta_{ref} T_{ref}\right] + \left(1 - \eta T,_{ref}\right)\right) T_{amb}}{\left(1 - \phi\left(1 - \beta_{ref}\eta T,_{ref}\right)\right)} \qquad \ldots\ldots\text{Equation 8}$$

Where,

$$\phi = \frac{\left(I \times A \times \alpha_{abs} \times \tau_{tran} \times \Sigma R_{th(f)} \times \Sigma R_{th(b)}\right)}{\left(\Sigma R_{th(f)} + \Sigma R_{th(b)}\right)}$$

The thermal resistance circuit of the system is illustrated in Figure 3. The calculation of the total thermal resistance for both the front and back sides will be explained in the subsequent subsections.
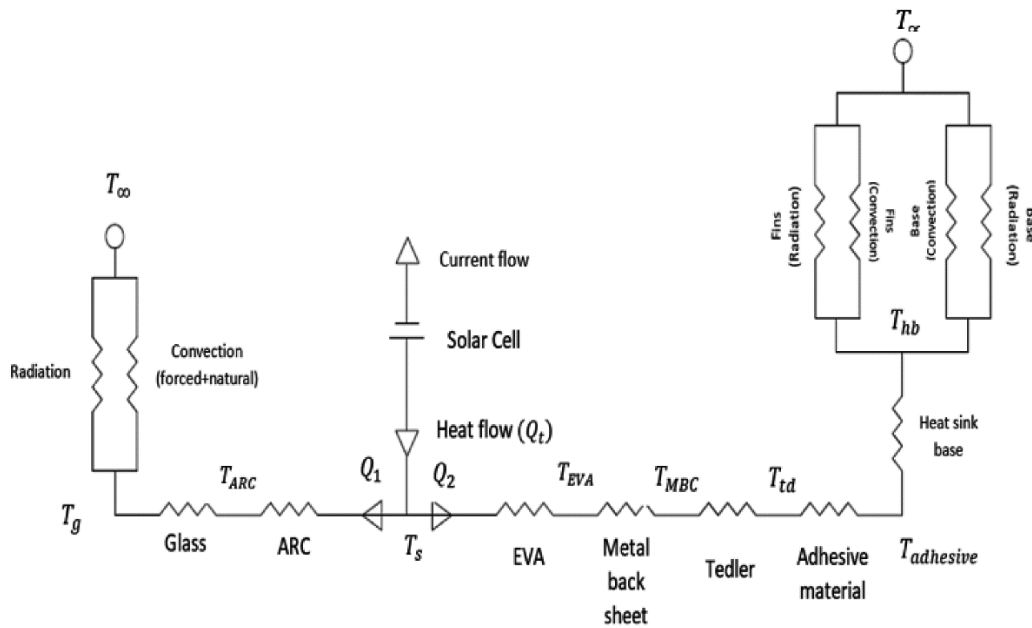

Figure 1: Thermal resistance circuit of the problem

4.1 Estimation of the Total Front Resistance

$$\Sigma R_{th(f)} = R_{tf} = R_{glass} + R_{ARC} + \frac{R_{radiation(r)} R_{convection(f)}}{R_{radiation(f)} + R_{convection(f)}} \qquad \ldots\ldots\text{Equation 9}$$

Where,

R_{glass} = is the resistance of the glass cover (Ω),

R_{ARC} = is the anti-reflective layer resistance,

$R_{radiation(f)}$ = is the radiation resistance on the front surface (Ω), and

$R_{convection(f)}$ = is the resistance of combined (forced and natural) convection on the front surface (Ω).

The

resistance of the glass cover (Ω) is calculated using:

$$R_{glass} = \frac{t_{glass}}{K_{glass} A_{glass}} \qquad \ldots\ldots\text{Equation 10}$$

Where:

K_{glass} = is the thermal conductivity of the glass material,

A_{glass} = is the area of the glass layer, and

t_{glass} = is the thickness of the glass layer.

Similarly, the thermal resistance of the anti-reflective layer defined as:

$$R_{ARC} = \frac{t_{ARC}}{K_{ARC}A_{ARC}}$$ ……Equation 11

Here,
K_{ARC} = represents the thermal conductivity of the anti-reflective layer, (W/m·K)
A_{ARC} = is the area of the anti-reflective layer, (m^2) and
t_{ARC} = is the thickness of the anti-reflective layer (m).

To account for radiation effects on the front surface of the solar panel, the radiation resistance is given by (Weiss, Amara et al., 2016):

$$R_{radiation} = \frac{1}{h_{radf} \times A}$$ ……Equation 12

Where:
h_{radf} = $4 \times \sigma \times \varepsilon_{si} \times (T_\infty)^3$,
ε_{si} = is the radiation heat transfer coefficient, and
A = is the surface area of the solar panel.
T_∞ = is the ambient temperature in (Singal, Saini et al.) and,
σ = is the Stefan-Boltzmann constant.

The combined resistance of forced and natural convection on the front surface can be calculated as:

$$R_{convection} = \frac{1}{h_f \times A}$$ ……Equation 13

Here, h_f represents the convective heat transfer coefficient, which is a combination of forced convection (h_{ff}) and natural convection (h_{fn}) coefficients and it can be estimated by (Kaplani and Kaplanis 2014)

$$h_f = \sqrt[3]{(h_{ff})^3 + (h_{fn})^3}$$ ……Equation 14

The forced convection coefficient h_{ff} can be determined using the equation:

$$h_{ff} = 0.848\, k \left[sin\, \beta\, cos\, u_w * \gamma * \frac{p_r}{u} \right]^{0.5} \left(\frac{L_{Ct}}{2} \right)^{-0.5}$$ ……Equation 15

Where:
k = is the thermal conductivity of the fluid,
h = is the heat transfer coefficient,
β = is the tilt angle of the solar panel,
u_w = is the wind velocity, (m/s)
γ = is the angle of wind speed,

P_r = is the Prandtl number,

L_{Ct} = is the characteristic length. (m)

The natural convection coefficient hfn can be expressed as:

$$h_{nf} = \frac{Nu_{fn} \times k}{L}$$ ……Equation 16

Where:

u = is the characteristic velocity, and

k = is the thermal conductivity of the fluid, and

L = is the characteristic length. (m)

Nu_{fn} = is the Nusselt number, number for front surface, and it can be calculated by (Álvarez, Xamán et al., 2008)

$$Nu_{fn} = \begin{cases} \left[0.13\left\{ (Ra)^{\frac{1}{3}} - (Gr_cP_r)^{\frac{1}{3}} \right\} + 0.56(Gr_cP_r sin\beta)^{\frac{1}{4}} \right]; if\ \beta > 30^o \\ \left[0.13\left\{ (Ra)^{\frac{1}{3}} \right\} \right];\ if\ \beta \leq 30^o \end{cases}$$ ……Equation 17

where Gr_c is the critical Grashof number and Ra is the Rayleigh number. They are given by:

Grc = 1.327 × 1010 exp{−3.708(π/2 − β)} ……Equation 18

$$R_a = \frac{g(T_{avg} - T_\infty)L_{ct}^3 P_r}{(0.25T_{avg} - 0.75T_\infty)v^3}$$ ……Equation 19

These equations allow for the calculation of the thermal resistances and coefficients involved in the heat transfer analysis of the solar panel system.

4.2 Estimation of the Total Back Resistance

The total back resistance ($\Sigma R_{th(b)}$) of the solar panel can be estimated using the following equation:

$$\Sigma R_{th(b)} = R_{tb} = R_{EVA} + R_{MBC} + R_{Tedlar} + R_{ad} + R_{hb} + \frac{R_{base} \times R_{fins}}{R_{base} + R_{fins}}$$ ……Equation 20

Where:

R_{EVA} = represents the resistance of the ethylene vinyl acetate (EVA) layer on the solar panel (Ω).

R_{MBC} = is the resistance of the sheet back metal of the solar panel (Ω).

R_{base} = is the resistance of the base of the fin for both radiation and convection.

R_{Tedlar} = is the resistance of the Tedlar polymer layer on the solar panel (Ω).

R_{ad} = is the resistance of the adhesive material (Ω).

R_{hb} = is the conductive resistance of the heat sink base (Ω).

R_{fins} = is the resistance of the base of the fin for both radiation and convection (Ω).

The resistance of the ethylene vinyl acetate (REVA) can be calculated as:

$$R_{EVA} = \frac{t_{EVA}}{K_{EVA}A_{EVA}}$$ ……Equation 21

Where;

K_{EVA} = is the thermal conductivity of the ethylene-vinyl acetate, (W/m)

A_{EVA} = is the area of the ethylene-vinyl acetate layer, and (m^2)

t_{EVA} = is the thickness of the ethylene-vinyl acetate layer (m).

The resistance of the sheet back metal (R_{MBC}) is given by:

$$R_{MBC} = \frac{t_{MBC}}{K_{MBC}A_{MBC}}$$ ......Equation 22

Here,

K_{MBC} = is the thermal conductivity of the back-sheet metal, (W/m·K)

A_{MBC} = is the area of the back-sheet metal, (m^2) and

t_{MBC} = is the thickness of the metal layer (m).

The resistance of the Tedlar polymer (R_{Tedlar}) can be expressed as:

$$R_{Tedlar} = \frac{t_{td}}{K_{td}A_{td}}$$ ......Equation 23

Where;

K_{td} = is the thermal conductivity of the Tedlar polymer, (W/m·K)

A_{td} = is the area of the Tedlar polymer layer, (m^2) and

t_{td} = is the thickness of the Tedlar polymer (m).

The resistance of the adhesive material (R_{ad}) is estimated as:

$$R_{ad} = \frac{t_{ad}}{K_{ad}A_{ad}}$$ ......Equation 24

Here,

K_{ad} = is the thermal conductivity of the adhesive material,

A_{ad} = is the area of the adhesive material, and tad is the thickness of the adhesive layer.

t_{ad} = is the thickness of the adhesive material (m)

The conductive resistance of the heat sink base (Rhb) is calculated using:

$$R_{hb} = \frac{t_{hb}}{K_{hb}A_{hb}}$$ ......Equation 25

Where;

K_{hb} = is the thermal conductivity of the heat sink base, (W/m·K)

A_{hb} = is the area of the heat sink base, (m2) and

t_{hb} = is the thickness of the heat sink base (m).

The resistance of the base of the fin (R_{base}) for both radiation and convection is given by:

$$R_{base} = \frac{R_{convection(base)} \times R_{radiation(base)}}{R_{convection(base)} \times R_{radiation(base)}}$$ ......Equation 26

Where:

$R_{convection(base)}$ = represents the resistance of combined (forced and natural) convection on the back surface (Ω), and

$R_{radiation(base)}$ = is the radiation resistance of the back surface (Ω).

The resistance of combined forced and natural convection on the back surface ($R_{convection(base)}$) is calculated as:

$$R_{convection(base)} = \frac{1}{h_{btot}A_b} \qquad \qquad \text{......Equation 27}$$

$$h_{btot} = \sqrt[3]{(h_{bn})^3 \times \left(h_{bf}\right)^3} \qquad \qquad \text{......Equation 28}$$

$$h_{bn} = \frac{0.02772 \times Nu_{bn}}{L} \qquad \qquad \text{......Equation 29}$$

$$h_{bf} = \begin{cases} 5.74w^{0.8} L_{ct}^{-0.2}; & if\ Ec/Lct\ \leq\ 0.05 \\ 5.74w^{0.8}L_{ct}^{-0.2} - 16.46\ L_{ct}^{-1}; & if\ 0.05\ <\ Ec/Lct\ <\ 0.95 \\ 3.83w^{0.5}L_{ct}^{-0.5}; & if\ Ec/Lct\ \geq\ 0.95 \end{cases} \qquad \text{......Equation 30}$$

Where;

h_{btot} = is the total heat transfer coefficient from the back, and

Nu_{bn} = is the natural Nusselt number from back surface

A_b = is the area of the base of the heat sink and is estimated by: $(L \times W) - (N \times t \times L)$.

The natural Nusselt number from back surface can be estimated by

$$Nu_{bn} = \begin{cases} 0.58(Ra)^{\frac{1}{5}}; & if\ \beta\ \leq\ 2^o \\ 0.58(Ra\ sin\beta)^{\frac{1}{5}}; & if\ 2^o\ <\ \beta\ <\ 30^o \\ \left[0.825 + \frac{0.387(Ra\ Sin\beta)^{1/6}}{\{1+(0.492/Pr)^{9/16}\}^{8/27}}\right]; & if\ \beta\ \geq\ 30^o \end{cases} \qquad \text{......Equation 31}$$

The radiation resistance of the back surface is

$$R_{radiation(base)} = \frac{1}{A_b \times h_{radback(base)}} \qquad \qquad \text{......Equation 32}$$

$$h_{radback(base)} = 4 \times \sigma \times \varepsilon_{alum} \times (T_\infty)^3 \times \left(1 - 2F_{base-fin}\right) \qquad \text{......Equation 33}$$

where ε_{alum} is the emissivity of the aluminum back in resistance. $F_{(fins-fins)}$ and $F_{(base-fin)}$ are the view factor of three-dimensional geometry and are given by:

$$F_{ij} = \frac{2}{\pi BU}\left(ln\left[\frac{(1+B^2)(1+U^2)}{1+B^2+U^2}\right]^{1/2} + B(1+U^2)^{1/2}tan^{-1}\frac{B}{(1+U^2)^{1/2}} + U(1+B^2)^{1/2}tan^{-1}\frac{U}{(1+B^2)^{1/2}} - \right.$$
$$\left. Btan^{-1}B - Utan^{-1}U\right) \qquad \qquad \text{......Equation 34}$$

where $B = \frac{l_f}{s}$, $U = \frac{L}{s}$,

here; l_f is the length of fin (m), L is the length of the solar panel (m), and s is the spacing between fins (m). The resistance of base of fin for both radiation and convection is given by:

$$R_{fins} = \frac{R_{convection(fins)} \times R_{radiation(fins)}}{R_{convection(fins)} \times R_{radiation(fins)}} \qquad \text{......Equation 35}$$

$R_{convection(fins)}$ and $R_{radiation(fins)}$ are given by;

$$R_{convection(fins)} = \frac{1}{h_{btot} \times N \times \eta_f \times A_f} \qquad \text{......Equation 36}$$

$$R_{radiation(fins)} = \frac{1}{h_{radback(fins)} \times N \times A_f} \qquad \text{......Equation 37}$$

where N is the number of fins, h_{btot} is the total heat transfer coefficient from the back, $h_{radback(fins)}$ is the radiation heat transfer coefficient of the base of the heat sink, and A_f is the area of a single fin. A_f and $h_{radback(fins)}$ are calculated by:

$$A_f = 2L \times \left[l_f + \frac{t}{2} \right] \qquad \text{......Equation 38}$$

$$h_{radback(fins)} = 4 \times \sigma \times \varepsilon_{alum} \times (T_\infty)^3 \times \left(1 - F_{fins-fins} - F_{fins-base} \right) \qquad \text{......Equation 39}$$

where L is the solar panel length (m), $F_{fin-base}$ is the view factor of fin-base, $F_{fins-fins}$ is the view factor of fins-fins, and η_f is the efficiency of the fins and is described as the ratio of the heat transfer to the fin to the heat transfer to an ideal fin under the adiabatic condition:

$$\eta_f = \frac{\tan h \, m \, L_c}{m \, L_c} \qquad \text{......Equation 40}$$

m is a constant and it is expressed as:

$$m = \sqrt{\frac{4h_{btot}}{kt}} \qquad \text{......Equation 41}$$

where h_{btot} is the total heat transfer coefficient from the back

L_c is characteristic length and is estimated by:

$$L_c = l_f + \frac{t}{2} \qquad \text{......Equation 42}$$

4.3 Estimation of the Solar Panel Efficiency and Produced Power

Once the solar panel temperature is obtained, the efficiency of the solar panel can be calculated using Equation (2), and the output power can be calculated using the following equation:

$$P = IA(1 - \eta)\alpha_{abs}\tau_{tran} \qquad \text{......Equation 43}$$

5. Results and discussion

The analytical model was validated by comparing its predictions with experimental data obtained from the literature. This validation process ensures that the model accurately represents the thermal behavior of the solar panel system. Additionally, the model was used to determine the optimum fin length that maximizes thermal performance.

After validation, the model was further utilized to investigate the influence of various parameters on the temperature of the solar panel. These parameters include:

1. Length and thickness of fins: By varying the length and thickness of the fins, the model can assess their impact on the solar panel temperature. This analysis helps determine the optimal dimensions of the fins for improved thermal performance.
2. Wind velocity: The model considers the effect of wind velocity on the convective heat transfer from the solar panel. By varying the wind velocity, the model can assess its influence on the temperature of the panel.
3. Tilt angle: The tilt angle of the solar panel affects the incident solar radiation and the convective heat transfer. The model can evaluate how different tilt angles impact the temperature of the panel.
4. Ambient temperature: The surrounding ambient temperature affects the heat dissipation from the solar panel. By changing the ambient temperature, the model can investigate its influence on the panel temperature.
5. Emissivity of the heat sink surface: The emissivity of the heat sink surface affects its radiation properties. By adjusting the emissivity value, the model can analyze its impact on the panel temperature.

Through these investigations, the model provides insights into the thermal behavior of the solar panel system and allows for the optimization of various parameters to enhance its overall performance. The results of these analyses are presented in the subsequent sections, providing valuable information for designing and operating solar panel systems efficiently.

5.1 Model Validation

To validate the developed analytical model, a comparison was made with indoor experimental results by Arifin, Tjahjana et al. (2020), which utilized a similar cooling method as the present study, as well as outdoor experimental results by Li, Ma et al. (2019) and Ahmad, Khandakar et al. (2018). The inputs used in these previous studies were also employed in the present study for result generation and validation purposes.

Table 2: Inputs used by some available experimental data in the literature.

Variables	Inputs Used by (Arifin Tjahjana et al., 2020)	Inputs Used by (Li, Ma et al., 2019)	Inputs Used by Ahmad, Khandakar et al.,2018)
Width	0.65 m	1 m	0.054 m
Length	0.67	2 m	1.19 m
Wind speed	1.5 m/s	Real variable values	Real variable values
Irradiation	-	Real variable values	Real variable values
Ambient temperature	25 ∘C	Real variable values	Real variable values
Length of fin	0.03 m	-	-
Thickness of fin	0.002 m	-	-

$$R^2 = \left[\frac{(\sum_{i=1}^{N}(y_i - z_i)^2 - \sum_{i=1}^{N}(x_i - y_i)^2)}{\sum_{i=1}^{N}(y_i - z_i)^2} \right]$$

$$RMSE = \left[\frac{\sum_{i=1}^{N}(y_i - x_i)^2}{N} \right]^{1/2}$$

$$Chi - square = \sum_{i=1}^{N} \frac{(x_i - y_i)^2}{y_i}$$

$$Maximum\ standard\ error = \sqrt{\frac{\sum_{x=1}^{N}(x_i - y_i)^2}{N-1}}$$

where (x_i), (y_i), and (z_i) are the experimental result, predicted result of the developed model, and mean of the experimental results, respectively.

Figure 4: This figure compares the impact of irradiance on solar panel temperature with and without a cooling system. The comparison includes the analytical model presented in this study and the experimental results reported by Arifin, Tjahjana et al. (2020). It indicates that for a solar panel without a cooling system, there is an excellent agreement between the two solutions. However, when a cooling system is added, there is a noticeable difference between the curves, especially at solar irradiances of 800 W/m^2 and above.
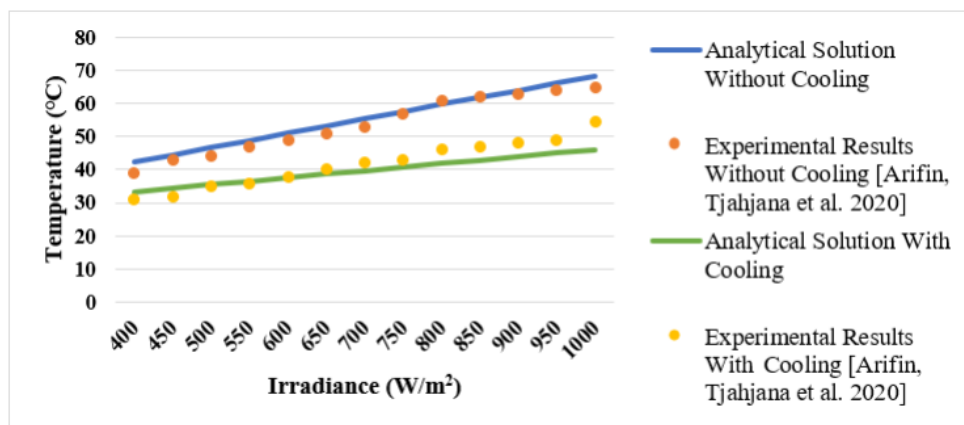

Figure 2: Model validation of the solar panel temperature compared with Arifin, Tjahjana et al. (2020)

Figure 5: This figure illustrates the variation of solar panel temperature during the daytime. It compares the experimental results presented by Li, Ma et al. (2019)with the predictions of the presented model. The curves exhibit a high degree of similarity and excellent agreement, validating the accuracy of the model in predicting the performance of a solar panel under real operating conditions.
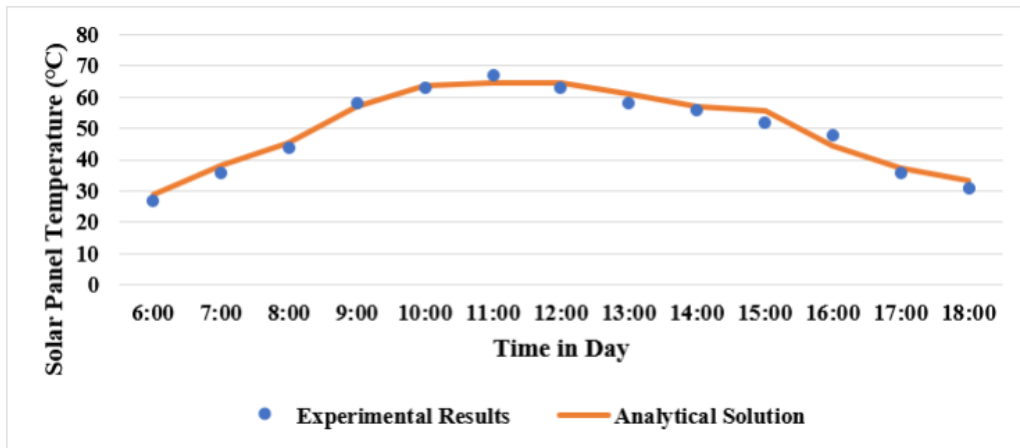
Figure 3: Model validation of the solar panel temperature compared with Li, Ma et al. (2019)

Figure 6: This figure compares the experimental results reported by Ahmad, Khandakar et al. (2018) with the results obtained from the developed model. The comparison specifically focuses on the scenario without a cooling system for certain hours during the daytime. The results demonstrate a good agreement between the experimental data and the predictions of the analytical model, thereby validating the accuracy and reliability of the presented model.
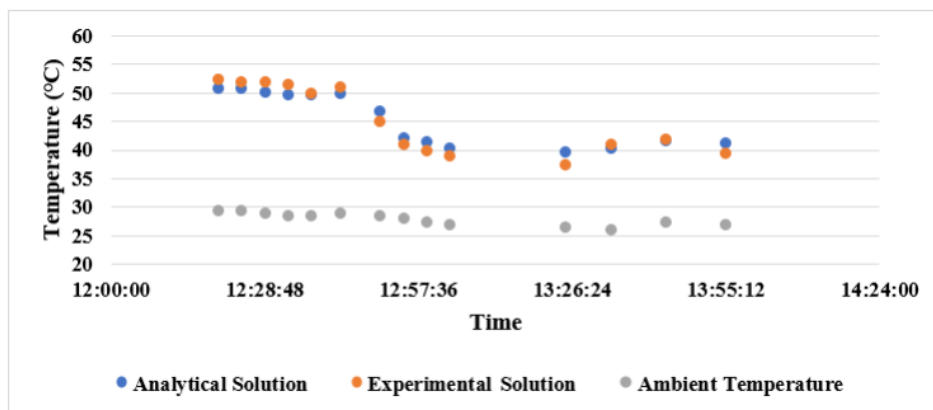

Figure 4: Model validation of the solar panel temperature compared with Ahmad, Khandakar et al. (2018)

6. Conclusions

The presented research work focuses on the development and optimization of a plate heat sink for passive cooling of a PV panel, aiming to improve its efficiency and lifespan. The study includes the following key aspects and findings:

a) **Analytical Model:** An analytical model was developed to predict the temperature, efficiency, and power output of the solar panel. The model takes into account various parameters such as the dimensions of the solar panel, fin length and thickness of the heat sink, wind speed, and ambient temperature. The model was successfully validated using real data from the literature.

b) **Optimal Fin Length:** The research investigated the optimal length of fins required for safe operation of the solar panel in a harsh desert environment. By considering worst-case environmental conditions, the study determined the fin length that ensures the solar panel operates below recommended

safe temperature levels.

7. References

1. Ahmad, H., Hariharan, N., Manirathnam, A. S., Vellingiri, S., & Mohankumar, R. S. (2014). CFD THERMAL ANALYSIS ON LAPTOP COOLING SYSTEM USING LOOP HEAT PIPE TECHNOLOGY International Journal of Research in Engineering and Technology, 2319–1163, 2321–7308. http://www.ijret.org

2. Ahmad, N.; Khandakar, A.; El-Tayeb, A.; Benhmed, K.; Iqbal, A.; Touati, F. Novel Design for Thermal Management of PV Cells in Harsh Environmental Conditions. Energies 2018, 11, 3231.

3. Alammar, A. A., Al-Dadah, R. K., & Mahmoud, S. M. (2016). Numerical investigation of effect of fill ratio and inclination angle on a thermosiphon heat pipe thermal performance. Applied Thermal Engineering, 108, 1055–1065. https://doi.org/10.1016/j.applthermaleng.2016.07.163

4. Arifin, Z.; Tjahjana, D.D.D.P.; Hadi, S.; Rachmanto, R.A.; Setyohandoko, G.; Sutanto, B. Numerical and Experimental Investigation of Air Cooling for Photovoltaic Panels Using Aluminum Heat Sinks. Int. J. Photoenergy 2020, 2020, 1574274.

5. Bar-Cohen, A.; Rohsenow, W.M. Thermally Optimum Spacing of Vertical, Natural Convection Cooled, Parallel Plates. J. Heat Transf. 1984, 106, 116–123.

6. Batalha Leoni, G., Suaiden Klein, T., & de Andrade Medronho, R. (2017). Assessment with computational fluid dynamics of the effects of baffle clearances on the shell side flow in a shell and tube heat exchanger. Applied Thermal Engineering, 112, 497–506. https://doi.org/10.1016/j.applthermaleng.2016.10.097

7. Calautit, J. K., & Hughes, B. R. (2016). A passive cooling wind catcher with heat pipe technology: CFD, wind tunnel and field-test analysis. Applied Energy, 162, 460–471. https://doi.org/10.1016/j.apenergy.2015.10.045

8. Calautit, J. K., Chaudhry, H. N., Hughes, B. R., & Ghani, S. A. (2013). Comparison between evaporative cooling and a heat pipe assisted thermal loop for a commercial wind tower in hot and dry climatic conditions. Applied Energy, 101, 740–755. https://doi.org/10.1016/j.apenergy.2012.07.034

9. Chiou, H. W., Lee, Y. M., Hsiao, H. H., & Cheng, L. C. (2017). Thermal modeling and design on smartphones with heat pipe cooling technique. IEEE/ACM International Conference on Computer-Aided Design, Digest of Technical Papers, ICCAD, 2017-November, 482–489. https://doi.org/10.1109/ICCAD.2017.8203816

10. Dubey, S.; Sarvaiya, J.N.; Seshadri, B. Temperature Dependent Photovoltaic (PV) Efficiency and Its Effect on PV Production in the World—A Review. Energy Procedia 2013, 33, 311–321.

11. Evans, D.; Florschuetz, L. Cost studies on terrestrial photovoltaic power systems with sunlight concentration. Sol. Energy 1977 19, 255–262.

12. Hassan Al-Ghazali, H., Wahhab. Aljibory, M., & Habeeb Alkharasani, T. (2018). Numerical and Experimental Study the Effect of Solid Particles Flow on Heat Pipe Performance. International Journal of Engineering & Technology, 7(4.30), 502. https://doi.org/10.14419/ijet.v7i4.30.25770

13. Hsiao, H. H., Chiou, H. W., & Lee, Y. M. (2019). Multi-angle bended heat pipe design using X-architecture routing with dynamic thermal weight on mobile devices. Proceedings of the Asia and South Pacific Design Automation Conference, ASP-DAC, 70–75. https://doi.org/10.1145/3287624.3287666

14. Huang, C. N., Lee, K. L., Tarau, C., Kamotani, Y., & Kharangate, C. R. (2021). Computational fluid dynamics model for a variable conductance thermosyphon. Case Studies in Thermal Engineering, 25(March), 100960. https://doi.org/10.1016/j.csite.2021.100960

15. Kaplani, E.; Kaplanis, S. Thermal modelling and experimental assessment of the dependence of PV module temperature on wind velocity and direction, module orientation and inclination. Sol. Energy 2014, 107, 443–460.

16. Li, Z.; Ma, T.; Zhao, J.; Song, A.; Cheng, Y. Experimental study and performance analysis on solar photovoltaic panel integrated with phase change material. Energy 2019, 178, 471–486.

17. Pawar, V. R., & Sobhansarbandi, S. (2020). CFD modeling of a thermal energy storage based heat pipe evacuated tube solar collector. Journal of Energy Storage, 30(January), 101528. https://doi.org/10.1016/j.est.2020.101528

18. Singal, S.; Saini, R.; Raghuvanshi, C. Analysis for cost estimation of low head run-of-river small hydropower schemes. Energy Sustain. Dev. 2010, 14, 117–126.

19. Soman, A., & Shastri, Y. (2015). Optimization of novel photobioreactor design using computational fluid dynamics. Applied Energy, 140, 246–255. https://doi.org/10.1016/j.apenergy.2014.11.072

20. Sözen, A., Gürü, M., Khanlari, A., & Çiftçi, E. (2019). Experimental and numerical study on enhancement of heat transfer characteristics of a heat pipe utilizing aqueous clinoptilolite nanofluid. Applied Thermal Engineering, 160(June), 114001. https://doi.org/10.1016/j.applthermaleng.2019.114001

21. U.S. Department of Energy. Solar Energy Technology Basics. 2013. Available online: https://www.energy.gov/eere/solar/ articles/solar-energy-technology-basics

22. Wang, J., Gan, Y., Liang, J., Tan, M., & Li, Y. (2019). Sensitivity analysis of factors influencing a heat pipe-based thermal management system for a battery module with cylindrical cells. Applied Thermal Engineering, 151(February), 475–485. https://doi.org/10.1016/j.applthermaleng.2019.02.036

23. Weiss, L.; Amara, M.; Ménézo, C. Impact of radiative-heat transfer on photovoltaic module temperature. Prog. Photovolt. Res.Appl. 2016, 24, 12–27.

24. Yue, C., Zhang, Q., Zhai, Z., & Ling, L. (2018). CFD simulation on the heat transfer and flow characteristics of a microchannel separate heat pipe under different filling ratios. Applied Thermal Engineering, 139, 25–34. https://doi.org/10.1016/j.applthermaleng.2018.01.011